Technical Paper

Bond and durability investigation of basalt fiber and PEN fiber reinforced composites for concrete applications

Donguk Choi, Youngho Kim*, Batzaya Baasankuu, Gombosuren Chinzorigt

Abstract: Bond and durability characteristics of basalt fiber reinforced polymer (BFRP) and polyethylene naphthalate (PEN) fiber/PEN FRP were investigated. Magnitude and distribution of the bond stress between BFRP/PEN FRP and concrete were investigated by double lap shear test. Four different types of durability test were performed: (1) Beam bond test following accelerated conditioning protocols by ACI 440.9R using plain concrete beams strengthened with BFRP or PEN FRP; (2) tensile test of PEN fiber/PEN FRP after immersion in 1N NaOH, 3% NaCl solutions, and water up to 6 months; (3) tensile test of PEN fiber/PEN FRP after immersion in 5% and 10% diluted solutions of HCl; and (4) exposure to natural outdoor environment. Bond test results indicated high bond stress developing over relatively short distance for BFRP that has high elastic modulus (E_{BF} = 68.4 GPa) while relatively low bond stress developing over longer length for PEN FRP that has low elastic modulus (E_{PEN} = 17.4 GPa). In the beam bond test, very good behavior was shown by PEN FRP after 4 month's exposure to wet and alkaline conditions while moderate behavior was shown by BFRP. Overall, the performance of PEN fiber/FRP was satisfactory in all durability tests conducted in this study.

Keywords: fiber reinforced polymer; double lap shear test; durability; beam bond test; basalt fiber; PEN fiber.

1. Introduction

Various fibers, including carbon fiber (CF), aramid fiber (AF), glass fiber (GF), and basalt fiber (BF), are used for the purpose of external strengthening of RC structures and members. The mechanical characteristics common to CF, AF, GF, and BF include linearly-elastic stress-strain relationship, high tensile strength, and high elastic modulus while they have relatively small rupture strain (< 3%). On the other hand, a new class of fiber including polyethylene terephthalate (PET) fiber and polyethylene naphthalate (PEN) fiber has non-linear stress-strain relationship, good strength in tension, low elastic modulus, and large strain capacity in tension (4%-15%): i.e. PET/PEN fibers are often said to have LRS (large rupture strain) capacity.

Donguk Choi is a Professor of School of Architecture and Design Convergence of Hankyong National University, Korea.
Corresponding author Youngho Kim is a Professor of Department of Chemical Engineering of Hankyong National University, Korea.
Batzaya Baasankuu is an Assistant Lecturer of Department of Civil Engineering and Architecture of Mongolian University of Science and Technology, Mongolia.
Gombosuren Chinzorigt is an Engineer at Gurvan Tahilgat Orgil LLC, Mongolia.

In this study, bond and durability characteristics of two different fibers were investigated: BF and PEN fiber. BF is an inorganic fiber produced from natural basalt rocks by melting and extrusion process [1, 2]. BF, which has been used in Civil Engineering discipline only recently, is more economical than CF or AF. Basalt fiber has excellent thermal resistance such that it can be used as insulating material replacing asbestos which poses health hazards by damaging respiratory systems [1]. PEN fiber is a synthetic fiber and is a product of petrochemical industry. PEN fiber has good strength (over 800 MPa) and low elastic modulus (about $1/4^{th}$ of BF), exhibits non-linear stress-strain behavior, and has large rupture strain in tension (7%-9%).

Thin BFRP sheets are often used for external strengthening in flexure and/or shear of RC beams [3, 4]. BFRP sheet or the basalt fiber rope can also be utilized for seismic strengthening of RC columns in the form of external wrapping [5-7]. Bond characteristics of BF bonded to concrete using adhesive have been investigated [8-10]. Shen et al. studied bond behavior of 21 test specimens by double lap shear test subjected to different strain rate. Effective bond length of BFRP ranged between 56-72 mm while the effective bond length decreased with the

increasing strain rate which varied between 70 mm/sec to 0.07 mm/sec [8]. Xie et al. studied the bond behavior BFRP-concrete interface subjected to wet-dry cycling in a marine environment using 26 small beams specimens [10]. The concrete beams were externally strengthened using BFRP sheet on the tension side. The test specimens were immersed in salt water with concentration of 3.5% and subjected to wet-dry cycles up to 360 days (one cycle per day). All beam specimens were tested by 4-point bending. For the control specimens, the failure mode was debonding of the adhesive layer before exposure while the failure mode changed to BFRP fracture in tension after exposure to marine environment. The fatigue strength of the BFRP/concrete interface after the wet-dry cycling was approximately 60% of the ultimate load capacity (of the control specimen). Existing durability test results of BFRP indicate that the BF may also degrade under wet and alkaline conditions [11]. The durability performance of BFRP can be improved by coating the BF with zirconium dioxide or titanium dioxide [12-14].

Recent research explored possible application of the LRS PET FRP and PEN FRP composites mainly for the external strengthening of the RC columns by confinement utilizing its large rupture strain capacity [15-20]. Baasankhuu et al. compared the behaviour of concrete cylinders confined by BFRP and PEN FRP [18]. The strength of confined concrete wrapped by PEN FRP was achieved at much higher axial/lateral strain of the concrete than the BFRP wrapping: PEN FRP wrapped concrete deformed more laterally to develop axial strength equivalent to BFRP wrapped concrete. Park et al. reported results of a rare study on the flexural strengthening of RC beams using PET FRP [21]. Despite very low elastic modulus (about 1/20th that of steel) of PET FRP, the external strengthening by 6-mm-thick multi-layer PET FRP sheet was effective to significantly improve the flexural strength and ductility of the RC beams. PET FRP sheet did not debond from the concrete substrate at ultimate.

At present, there are few studies that focused on the bond behavior between LRS PEN FRP and concrete. In addition, few studies can be found in the existing literature either on the durability characteristics of PEN FRP clearly indicating a research need. One objective of this study was to investigate and compare the bond behavior of BFRP-to-concrete and PEN FRP-to-concrete interfaces in terms of magnitude and distribution of the bond stress. Bond behavior was investigated by double lap shear test in this study. The other objective was to investigate the durability characteristics of BFRP, PEN fiber/PEN FRP. Four different durability tests were performed: (1) beam bond test by accelerated conditioning protocols (ACP) by ACI 440.9R for both BFRP and PEN FRP; (2) durability test of PET fiber/FRP under wet, saline, alkaline conditions up to 6 months; (3) durability test of PET fiber/FRP under acidic conditions; and (4) exposure to natural outdoor conditions. The durability test program especially concentrated on the PEN fiber/FRP.

Table 1 Mechanical properties of fiber roving and adhesive

Type	Stress (MPa)	Strain (%)	E_1 (GPa)	E_2 (GPa)	Area (mm^2)	Thickness (mm)	Density (g/mm^3)
Basalt fiber roving	1226	1.95	68.4	n/a	0.45	0.113	0.0027
PEN fiber roving	822	8.03	17.4	8.30	2.00	0.840	0.0014
PEN fiber sheet	842	9.01	17.5	8.33	--	--	--
PEN FRP	912	9.13	21.4	8.59	--	--	--
Adhesive	40.9	2.58	1.59	--	--	--	--

NOTE: 1. Results show mean value of 12 tests for fibers and 5 tests for adhesive; 2. PEN fiber shows bilinear response and so the slope of the first and the second line is shown as E_1 and E_2, respectively (see Fig. 1(b)); 3. Adhesive mechanical properties were tested 7 days after hardening.

2. Material properties and test method

2.1 Material properties of fibers and adhesive

Tensile properties of BF roving, PEN fiber roving, PEN fiber sheet, and PEN FRP (i.e. PEN fiber sheet embedded by two-part epoxy) were tested following ISO 10406-2 with results summarized in Table 1 [22]. Twelve tensile tests were completed for each fiber/FRP while the mean values are shown in Table 1. Figure 1(a) shows the stress-strain relationship of BF and PEN fiber determined in this study. In Figure 1(a), the stress-strain relationship is linear for BF while it is non-linear for PEN fiber. The non-linear stress-strain relationship of PEN fiber can be modelled using a bilinear relationship with each line having a slope of E_1 (slope of the first line connecting the origin and the stress corresponding to 1% strain) and E_2 (slope of the second line), respectively, as shown in Table 1 and Fig. 1(b). For the double lap

shear test, beam bond test, and tensile test of the BFRP and PEN FRP, a two-part epoxy (adhesive) was used. The tensile properties of the adhesive were determined following ASTM D638 [23]. As shown in Table 1, tensile strength, ultimate strain in tension, and elastic modulus of the adhesive are 40.9 MPa, 2.58%, and 1.59 GPa, respectively. A universal testing machine (UTM) of 50-kN capacity was used for tensile tests of fibers/FRP and adhesive.
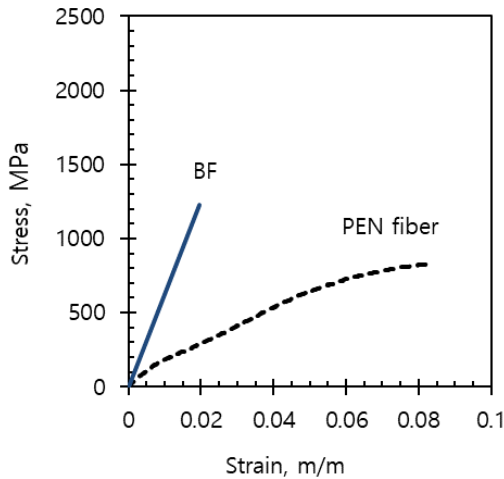
(a) Stress-strain relationship
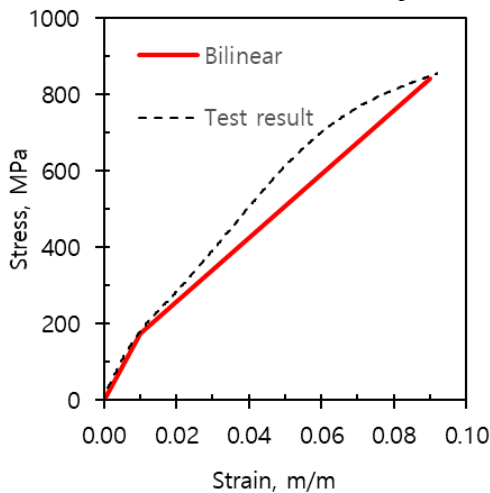
(b) Bi-linear model of PEN fiber

Fig. 1 Stress-strain relationship of BF and PEN fibers

2.2 Double lap shear test

As the LRS PEN fiber has low elastic modulus, a significant thickness of the PEN FRP is needed when strengthening RC members such as RC beams, columns, etc. [18]. Bond stress that develops at the interface between the thick PEN FRP layer and the concrete substrate can be high because a thicker FRP may induce higher bond stress, which in turn may lead to a premature debonding failure at the FRP-concrete interface [24, 25]. Bond investigation by double lap shear test was planned both for the PEN FRP- and the BFRP-strengthened concrete specimens to investigate magnitude and distribution of the bond stress that develops between the FRP and the concrete.

Modified double lap shear test setup was used following recommendations of CSA S 806 Annex P in general [26]. Figure 2 shows a double lap shear test specimen used in this study. Size of the test specimen was 140 (b) x 150 (h) x 550 mm (L). Concrete with 30-MPa target strength was designed, cast in the laboratory, and wet cured for 28 days. The 28-day compressive strength was 36.0 MPa. A thin steel plate placed at center of specimen at time of casting practically disconnected a specimen into two concrete blocks of equal length. A 16-mm diameter grooved steel rod was installed in the middle of each concrete block in the axial direction with about 300-mm length protruding outside the concrete block (for use by testing grip of UTM). 28 days after casting, two opposing side faces of the concrete blocks were lightly roughened using a hand grinder. Two layers of BF rovings or single layer of PEN fiber sheet was applied (b_{FRP} = 100 mm, L_{FRP} = 500 mm), respectively, on the roughened faces using the adhesive with amount of 200% by vol. for BFRP and 150% by vol. for PEN FRP (The same amount of adhesive was used for BFRP and PEN FRP, respectively, throughout this study). Seven days after application of the adhesive, multiple 5-mm-long electronic strain gauges were installed on the surface of BFRP and PEN FRP starting from center of the specimen at 21-mm spacing on center as shown in Fig. 2.

Table 2 Test variables of double lap shear test

Type	No. of layers	No. of test	f_{ck} (MPa)	Fiber thk. (mm)	Adhesive thk. (mm)
BFRP	2	2	36.0	0.226	0.452
PEN FRP	1	2	36.0	0.840	1.260

The double lap shear test specimen was subjected to tensile force during test using 1,200-kN-capacity UTM operated in displacement control (ramp rate = 1 mm/min). The applied load was measured using load cell of the UTM. Signals from the strain gauges and the load cell were electronically recorded by a data logger. Two replicate specimens were tested for each FRP type. Table 2 summarizes test variables of the double lap shear test.
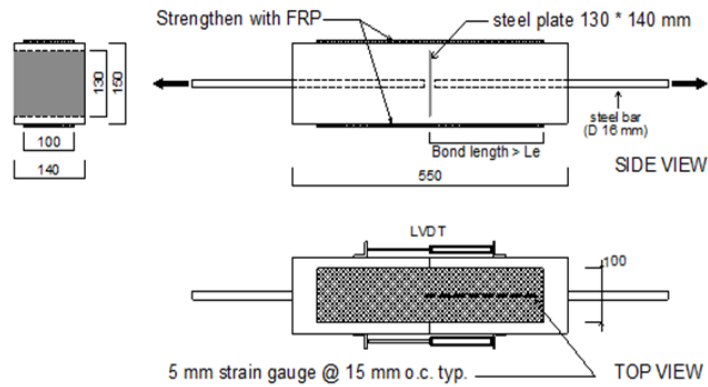
Fig. 2 Double lap shear test specimen [21]

2.3 Beam bond test

100 (*b*) x 100 (*h*) x 400 (*L*) mm plain concrete beam specimens were used for the beam bond test following guide to accelerated conditioning protocols (ACP) of durability assessment by ACI 440.9R [27]. Concrete with 60-MPa compressive strength was cast in the laboratory and wet cured for 28 days. A 50 x 100 mm acrylic plate (thickness = 2 mm) was inserted in the beam mid-span on the tension side up to beam half-height to create a notch as shown in Fig. 4(a). After 28 days of wet cure, two layers of BF rovings or single PEN fiber sheet was externally bonded on the bottom surface of the beam using adhesive. Concrete surface was lightly roughened before the FRP application. Both BFRP and PEN FRP were 80 mm wide and 200 mm long (See Fig. 4(a)). A week after the FRP application, the specimens were subjected to three different environmental conditions: Room condition (*T* = 23°C +/- 3°C) and immersion in water and 1N NaOH solutions, respectively (Temperature of water and NaOH solution = 60°C +/- 3°C). After immersion for 3,000 hours (4-months) in water and in the alkaline solution, the beams were retrieved and stored in the room condition for two days. Flexure test by three-point loading

following recommendations of ACI 440.9R was carried out using a 1,200-kN UTM at ramp rate of 0.6 mm/min as shown in Fig. 4 [27]. Five replicate beams were tested for the BFRP- and the PEN FRP-strengthened beams, respectively.

A small strip of BFRP or the PEN FRP was adhered using adhesive to one end of all beam bond specimens as shown in Fig. 3(c). After completion of the beam bond tests, the BFRP or PEN FRP strip attached at the end were subjected to pull-off test using a pull-off testing device equipped with a 50 x 50 mm square steel end plate. The steel end plate was adhered to the BFRP or PEN FRP strip using two-part epoxy after the FRPs were cut to fit 50 mm x 50 mm steel end plate (See Fig. 5). Seven days after the adhesive application, the pull-off test was performed as shown in Fig. 5(d). Average bond stress in tension was determined by dividing the maximum pull-off load (P_{max}) by the contact area ($A = 2,500$ mm^2). The pull-off test results of the FRPs retrieved from the specimens immersed in water and 1N NaOH solution and those stored in the room condition were compared.
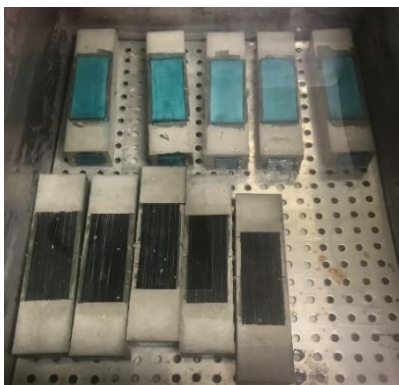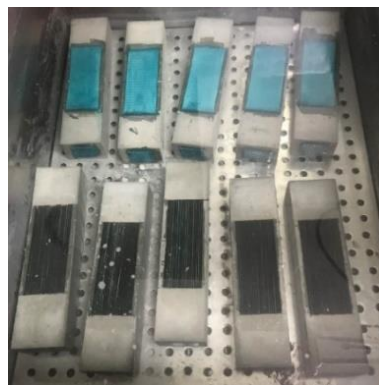
| (a) Water | (b) 1N NaOH | (c) Room condition |

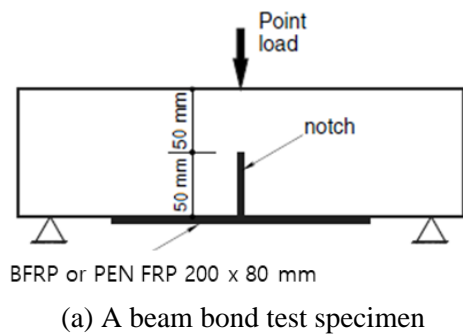Fig. 3 Beam bond test specimens immersed in water/alkaline solutions and stored in room condition

(a) A beam bond test specimen

(b) Beam bond test in progress

Fig. 4 Beam bond test setup

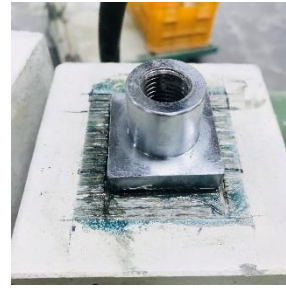(a) PEN FRP   (b) BFRP   (c) Steel end plate   (d) Pull-off test
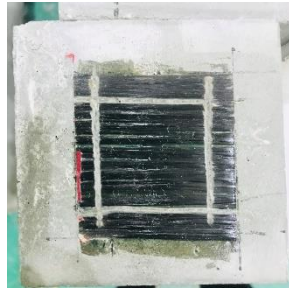
Fig. 5 Pull-off test

2.4 Tensile test of PEN fiber/FRP before/after exposure to NaOH/NaCl solutions and water

In this phase of study, durability characteristics of PEN fiber/FRP (i.e. Uniaxial PEN fiber sheet and PEN FRP) were investigated by observing weight change and change in the tensile properties before and after exposure to different environmental conditions up to 6 months. Multiple PEN fiber/FRP tensile specimens were prepared in length of 400 mm (PEN fiber sheet) or 300 mm (PEN FRP). Test specimens were immersed in three different environments: i.e. Water (i.e. 100% R.H. at 40°C) and 3% NaCl and 1N NaOH solutions at 20°C, respectively. The above environmental conditions simulated completely wet condition, seawater, and sound concrete with high alkalinity, respectively.

The weight measurement and the tensile test were carried out before the durability test began and after immersion for 1, 3, and 6 months to determine the weight loss and the strength/stiffness loss in tension, if any. After each planned immersion period, test specimens were taken out of the environmental chamber and dried for two days in a container about quarter full of silica gel. After the specimens were dried, they were weighed using a high precision scale (accuracy = 0.0001 g) and then the tensile test was performed following ISO 10406-2 (ten tests each). Scanning electron microscopy (SEM) photos were taken before/after the planned immersion period. Figure 6 shows PEN fiber sheet and PEN FRP specimens immersed in NaOH, NaCl solutions, or water.

(a) PEN fiber sheet

(b) PEN FRP

Fig. 6 PEN fiber/FRP specimens immersed in NaOH/NaCl solutions or water

2.5 PEN fiber/FRP immersion in diluted acidic solution

This specific durability test by tensile testing after immersion in acidic solution was carried out only for PEN fiber/FRP. Tensile test coupons consisted of PEN fiber sheet and PEN FRP, which were immersed in diluted acidic solutions of 5% HCl or 10% HCl for 3, 7, and 14 days. After the planned immersion period, the specimens were retrieved, dried for 2 days and subjected to tensile test. Tensile strength after immersion in diluted acidic solution was compared to that of the control specimen. Three replicate specimens were tested.

2.6 Exposure in natural environment for PEN fiber/FRP

This test was carried out for PEN fiber/FRP only. PEN fiber sheet and PEN FRP tensile test specimens were prepared which were exposed in the outdoor conditions in South Korea starting from late winter (T = 0°C ~ -10°C, R.H. = 30%-40% typ.) to early summer (T = 20°C-30°C, R.H. = 40%-60% typ.). After six-months' exposure in the natural environment including direct sun ray and U.V., the specimens were retrieved and subjected to tensile test. Change of tensile strength before/after exposure was examined using ten replicate specimens of PEN fiber/FRP, respectively.

3. Test results

3.1 Double lap shear test results

The double lap shear test was performed using two different FRP composites adhered to concrete: BFRP (2 layers) and PEN FRP (1 layer). Figure 7 schematically shows the location of the strain gauges attached on the surface of FRP and the force acting on FRP at center and in between the strain gauge locations. As soon as a test specimen shown in Fig. 2 is subjected to tensile force P, the concrete is separated into two parts due to a thin steel plate placed at center and, as a result, each FRP sheet bonded on the side face of the concrete block is subject to a tensile force of $P/2$ at center (loading end). Bond stress (u) acting at FRP-concrete interface between i^{th} and

$(i+1)^{th}$ strain gauges in Fig. 7 can be determined from Eqs. (1) through (4), where the stress is determined from strain readings of the strain gauge:

$$T^i = \sigma_x^i(ty). \quad \dots\dots\dots\dots \text{ (1)}$$
$$T^{i+1} = \sigma_x^{i+1}(ty) \dots\dots\dots\text{ (2)}$$
$$\Delta T = T^i - T^{i+1} \dots\dots\dots\dots\text{.(3)}$$
$$u = \frac{\Delta T}{xy} \dots\dots\dots\dots\dots\text{...(4)}$$

Where T^i = tensile force acting on FRP at i^{th} strain gauge, σ_x^i = axial stress of FRP at i^{th} strain gauge location, t = thickness of FRP, x = distance between two adjacent strain gauges, y = width of FRP.

Table 3 summarizes the maximum axial strain observed by the measured strain ($\varepsilon_{x\text{-}frp}$), corresponding axial stress ($\sigma_{x\text{-}frp}$), tensile force acting on the FRP layer (P_{frp}), and the maximum bond stress (u_{max}) determined by Eqs. (1) through (4). Figures 8 and 9 show distribution of axial strains and bond stresses for 126-mm distance starting from center for BFRP and PEN FRP, respectively. It is observed from Table 3 and Fig. 8 that the maximum axial strain, axial stress, in Table 3 and Fig. 9, the maximum axial strain, axial stress, FRP tensile force, and bond stress are 0.7%, 149 MPa, 15.1 kN, and 3.0 MPa, respectively, for PEN FRP-1 while they are 0.82%, 172 MPa, 17.4 kN, and 4.3 MPa for PEN FRP-2. The distance the bond stress develops (L_e) is 63-84 mm for BFRP while it is 105 mm for PEN FRP. The distance the bond stress develops as shown in Figs. 8 and 9 and Table 3 is known as the effective bond length L_e in literature: i.e. even if the bond length of the FRP is larger than L_e, the bond stress still develops within L_e. It can be seen that the effective bond length of BFRP (63-84 mm) determined in this study agrees well with that suggested by Shen et al., where the effective bond length varied between 56-72mm depending on the strain rate [8]. The bond stress between BFRP and concrete at the interface is relatively high and narrowly distributed as shown in Fig. 8 and Table 3. On the other hand, the bond stress is rather low and distributed over a larger distance for PEN FRP in Fig. 9 and Table 3. In all tests, the failure mode was debonding at the FRP-concrete interface as shown in Fig. 10 and Table 3.
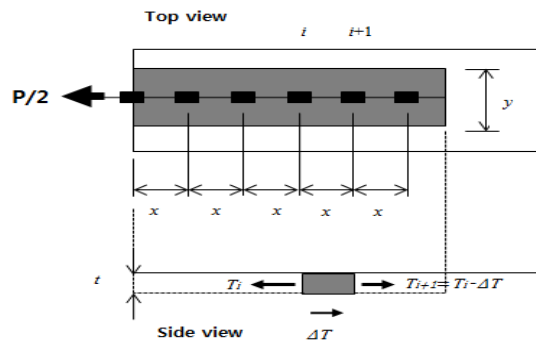

Fig. 7 Force ($P/2$) acting at center and away from center [21]

Table 3 Summary of test results at maximum fiber strain ($\varepsilon_{x\text{-}frp}$)
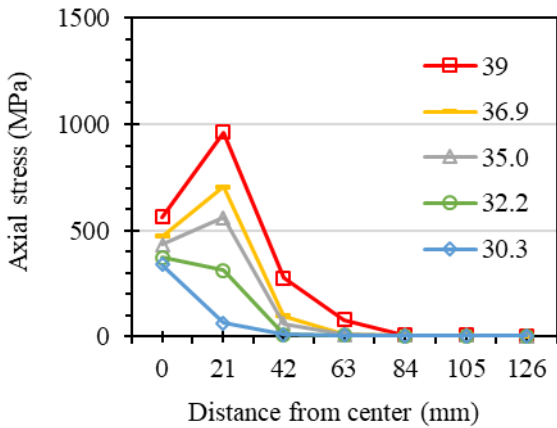
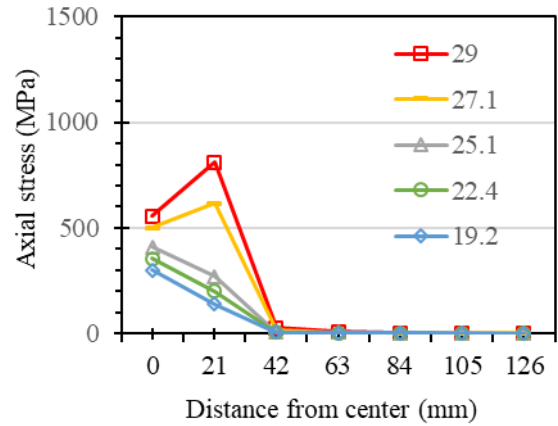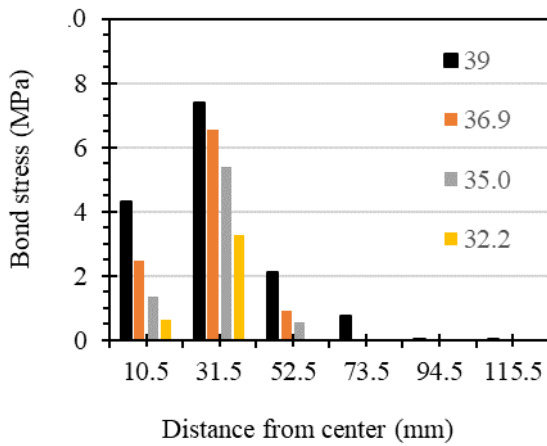| Fiber type	$\varepsilon_{x\text{-}frp}$	$\sigma_{x\text{-}frp}$ (MPa)	A_{frp} (mm^2)	P_{frp} (kN)	L_e (mm)	u_{max} (MPa)	u_{mean} (MPa)	u_{max} / u_{mean}	Failure mode
BFRP-1	0.0141	963	22.6	21.8	84	7.4	2.16	3.4	debonding
BFRP-2	0.0119	812	22.6	18.4	63	8.4	3.50	2.4	debonding
PEN FRP-1	0.0070	149	84.3	15.1	105	3.0	1.20	2.5	debonding
PEN FRP-2	0.0082	172	84.3	17.4	105	4.3	1.38	3.1	debonding
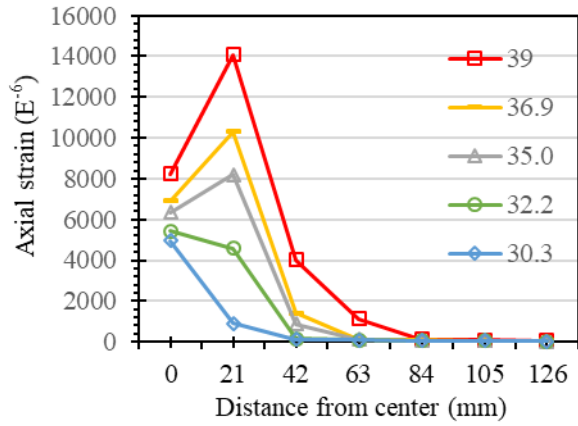
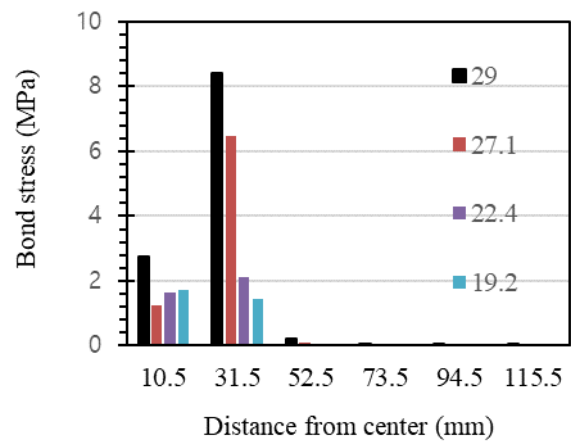(a) BFRP-1
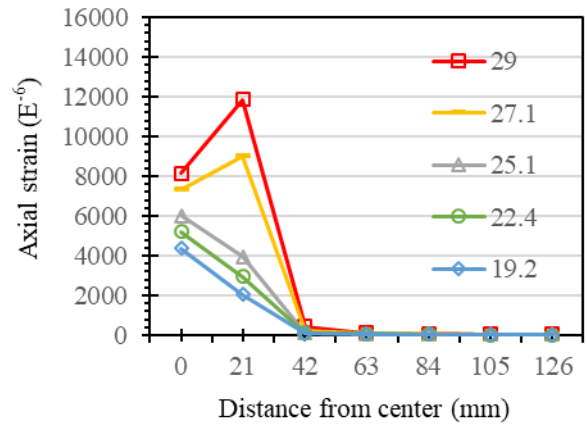
(a) BFRP-2

(b) BFRP-1

(b) BFRP-2

(c) BFRP-1

(c) BFRP-2

Fig. 8 Distribution of axial strain, axial stress, and bond stress at varying level of BFRP tensile force
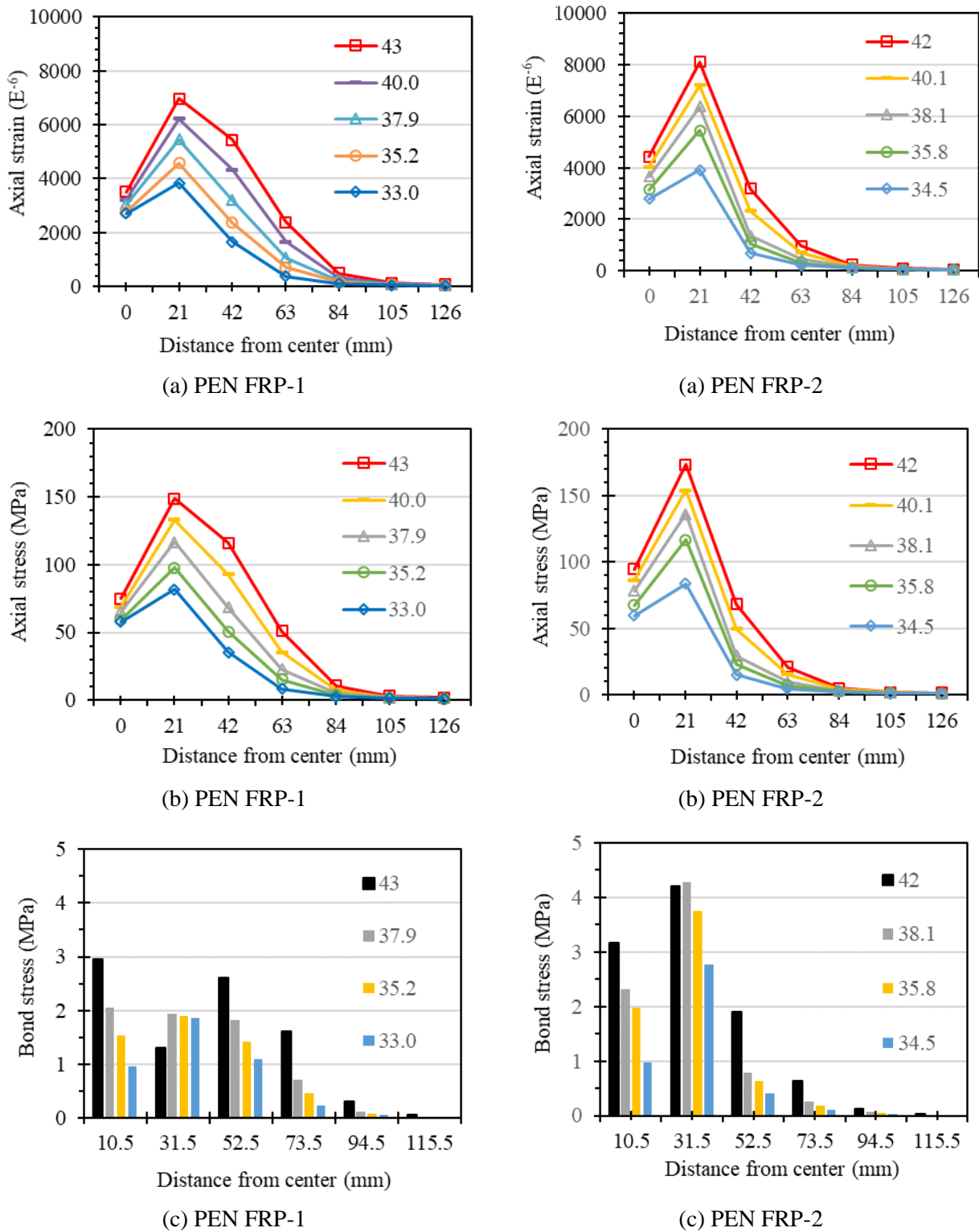
(a) PEN FRP-1

(a) PEN FRP-2

(b) PEN FRP-1

(b) PEN FRP-2

(c) PEN FRP-1

(c) PEN FRP-2

Fig. 9 Distribution of axial strain, axial stress, and bond stress at varying level of PEN FRP tensile force

3.2 Beam-bond test results of BFRP and PEN FRP

The beam bond test specimens were retrieved after 4-months' immersion in water or alkaline solution (1N NaOH) as well as the control specimens (stored in room condition for 4 months) and tested by flexure test by three-point loading following ACI 440.9R [27]. As the applied load increased, a tensile crack quickly appeared and developed upward starting from top of the notch (See Fig. 4). At peak load, BFRP- and PEN FRP-strengthened beams failed either by debonding at the FRP-concrete interface or FRP fracture in tension. Average peak load of C-BFRP (Control), RH-BFRP (R.H. 100%), and NaOH-BFP (1N NaOH) was 15.5 kN, 15.7 kN, and 7.94 kN, respectively, as shown in Table 4. Average peak load for C-PEN FRP, RH-PEN FRP, and

NaOH-PEN FRP was 19.7 kN, 17.4 kN, and 17.4 kN, respectively. Equation (5) was used to determine beam bond retention (or residual mechanical property) as suggested by ACI 440.9R [27].

$$R_{eb} = \frac{P_{b2}}{P_{b1}} \times 100 \ \ (\%)\ldots\ldots\ldots\ (5)$$

Where, P_{b2} is peak load of water/alkali conditioned specimen, P_{b1} is peak load of Control specimen and R_{eb} is beam is beam bond retention.

Table 4 Results of beam bond and pull-off tests

Index	Beam bond test		Pull-off	Index	Beam bond test		Pull-off
	Load (kN)	R_{eb} (%)	Test (MPa)		Load (kN)	R_{eb} (%)	Test (MPa)
C-BFRP	15.5	--	5.23	C-PEN FRP	19.7	--	4.47
RH-BFRP	15.7	100	3.97	RH-PEN FRP	17.4	88	3.56
NaOH-BFRP	7.94	51.2	3.55	NaOH-PEN FRP	17.4	88	1.90

NOTE: Results shown are average of 5 tests.

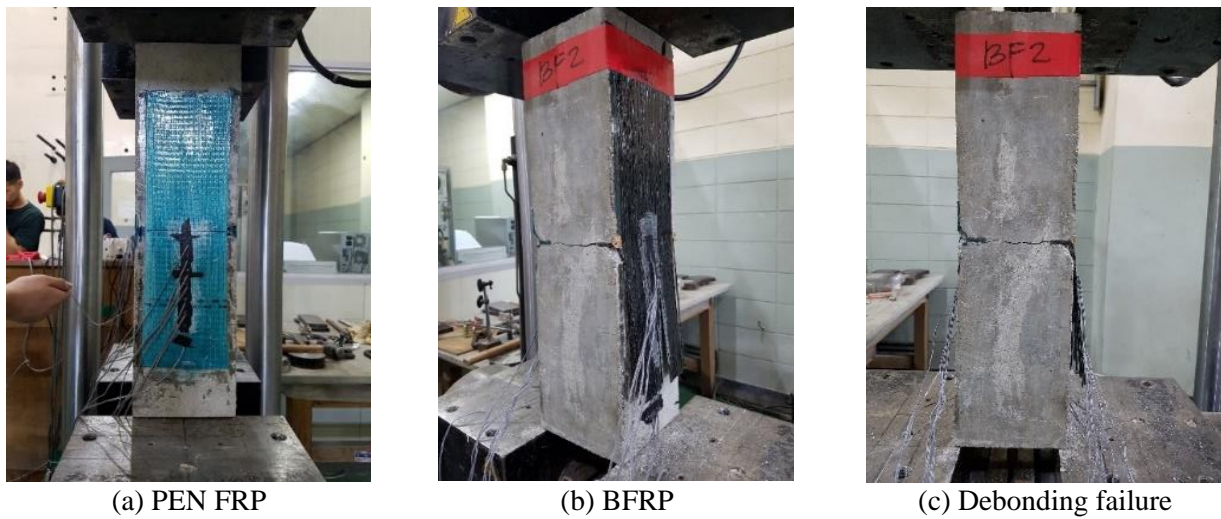(a) PEN FRP   (b) BFRP   (c) Debonding failure

Fig. 10 Double lap shear test in progress and failure mode

Table 4 summarizes the beam bond test results in terms of peak load and beam bond retention. The beam bond retention is 88% for PEN FRP both for wet condition and in alkaline condition. On the other hand, the beam bond retention is 100% and 51% in wet condition and in alkaline condition, respectively, for BFRP. Test results indicate that BFRP may be vulnerable for alkaline exposure. Figures 11 and 12 show the beam bond test specimens after test. In Figure 11 which shows the control specimens, the failure occurred at the FRP-concrete interface both for BFRP and PEN FRP. C-PEN FRP shows some concrete attached to the debonded FRP surface while C-BFRP shows almost complete and clean interface failure. Figure 12 shows top surfaces of C-BFRP, RH-BFRP, and NaOH-BFRP after beam bond test. C-BFRP retains original dark brown color of the BFRP in Fig. 12(a). On the other hand, yellowish discoloration of BFRP is shown for RH-BFRP in Fig. 12(b) while the discoloration is more severe for NaOH-BFRP in Fig. 12(c). It has been reported that the basalt fiber can be degraded under soaked, saline, and alkaline environment while the degradation of the basalt fiber can be significantly slowed down by

oxide coating such as zirconium deoxide and titanium deoxide coating [12-14]. Since the basalt fibers used in this study were not coated, further investigation on the durability properties of the basalt fiber was not pursued.

As described in Clause 2.3, the pull-off test of BFRP or PEN FRP bonded to the end of the beam bond test specimens was also performed after the completion of the beam bond test. Table 4 and Figures 13 and 14 show the results of pull-off test. Pull-off test results indicate that both immersion in water and alkaline solution at an elevated temperature tend to degrade the bond between concrete and BFRP/PEN FRP. C-BFRP (Control), RH-BFRP, and NaOH-BFRP have average pull-off bond strength of 5.23 MPa, 3.97 MPa, and 3.55 MPa, respectively, in Table 4, while average bond strength of C-PEN FRP (Control), RH-PEN FRP, and NaOH-PEN FRP is 4.47 MPa, 3.56 MPa, and 1.90 MPa, respectively. C-BFRP specimens failed mostly in concrete substrate while NaOH-BFRP specimens failed partially in concrete substrate. RH-BFRP specimens failed mostly at interface. PEN FRP pull-off specimens show partial failure at interface and concrete substrate for C-PEN FRP, and clean interface failure for

RH-PEN FRP and NaOH-PEN FRP specimens indicating damage at the interface by 4-months' immersion in water and alkaline solutions.

3.3 Test results of PEN fiber/FRP before/after exposure to NaOH, NaCl solutions and water

Table 5 compares the weights/weight losses before and after 30, 90, and 180 days of exposure for PEN fiber sheet and PEN FRP under three different conditions of completely wet (Wet, 40°C) and 3% NaCl and 1N NaOH solutions (20°C), respectively. In Table 5, PEN fiber sheet shows 0.33%, 0.18%, and 10.5% weight loss after exposure to Wet, NaCl, and NaOH conditions, respectively, while the loss is 0.80%, 0.76%, and 4.34% for PEN FRP, respectively, after 180 days. PEN fiber shows some negative effect under alkaline environment. However, the possible negative effect of alkaline environment on PEN fiber is significantly reduced in case of PEN FRP as the PEN fiber is embedded in the adhesive matrix.
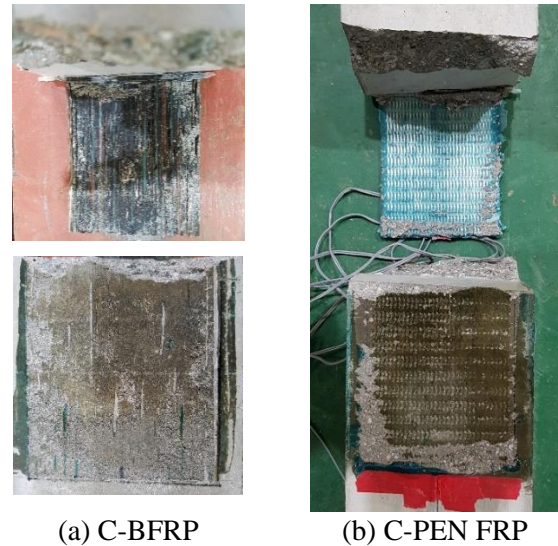

(a) C-BFRP   (b) C-PEN FRP

Fig. 11 Control specimens after beam bond test

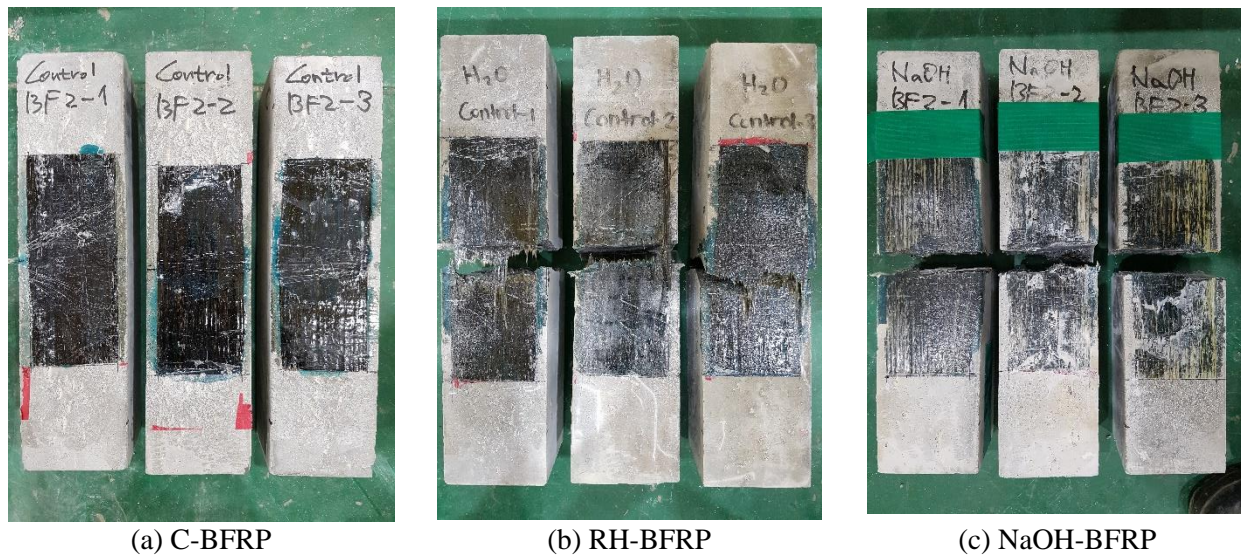(a) C-BFRP   (b) RH-BFRP   (c) NaOH-BFRP

Fig. 12 BFRP specimens after beam bond test

Table 6 summarizes the tensile test results for PEN fiber sheet and PEN FRP in terms of tensile strength and elastic modulus before and after 30, 90, and 180 days. In Table 6, the tensile strength of PEN fiber sheet after 180 days is 114%, 115%, and 97% of control when exposed to Wet, 3% NaCl, and 1N NaOH conditions, respectively. The tensile strength for PEN FRP after 180 days is 98%, 96%, 93% for Wet, 3% NaCl, and 1N NaOH conditions, respectively. Elastic modulus is also shown in Table 6. The elastic modulus (E_1) after 180 days ranges 98%-103% for PEN fiber sheet and 100%-104% for PEN FRP, respectively. It can be concluded that the PEN fiber/FRP has satisfactory resistance after exposure to all three environmental conditions of Wet, 3% NaCl, and 1N NaOH after 180 days.

Figure 15 shows SEM images before and after 180 days of exposure to different environmental conditions, where no significant change is visible before/after exposure. In Figure 15(a), the longitudinal surface of PEN fiber filament is very smooth and clean while the diameter is 30 μm before exposure. In Figure 15(b)-(d), after 180 days' exposure to wet, saline, and alkaline conditions, the surfaces do not show any significant trace of chemical etching or bruises in all conditions.

3.4 Influence of acidic condition

Figure 16 compares the test results of PEN fiber/FRP before and after immersion in 5% and 10% diluted solutions of HCl for 3, 7, and 14 days: i.e. Tensile strengths after immersion are normalized in terms of tensile strength before immersion in Fig. 16. It is seen in Fig. 16(a) that the tensile strength of PEN fiber sheet after immersion tends to be affected a little, while the tensile strengths are almost unaffected in Fig. 16(b) for PEN FRP specimens.

3.5 Exposure to natural environment

As described earlier, PEN fiber sheet and PEN FRP tensile test specimens were prepared and exposed in natural outdoor conditions for six months. Tensile test results are summarized in Table 7 after six months' exposure in the natural environment including direct sun ray and U.V. Degradation is clearly noticed for PEN fiber sheet while the degradation is significantly reduced for PEN FRP in Table 7.
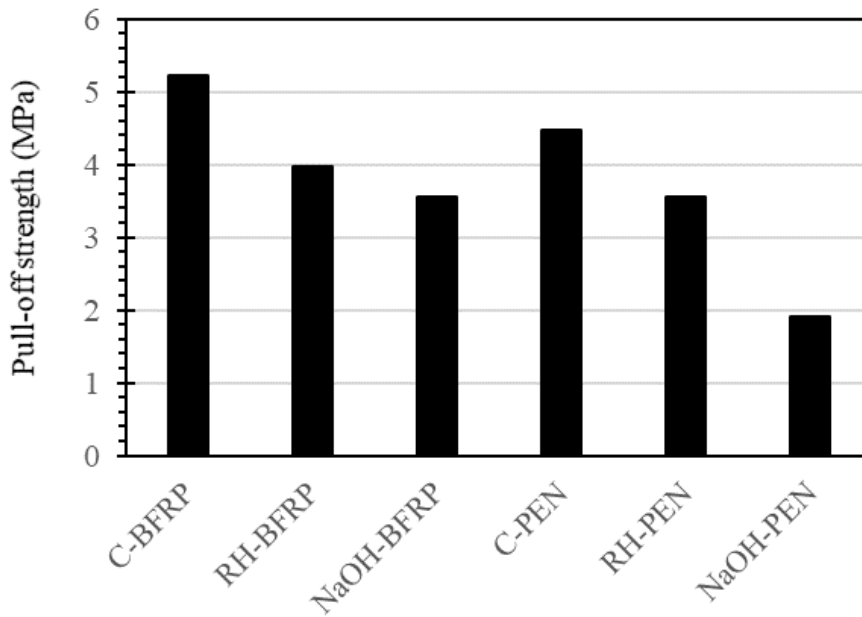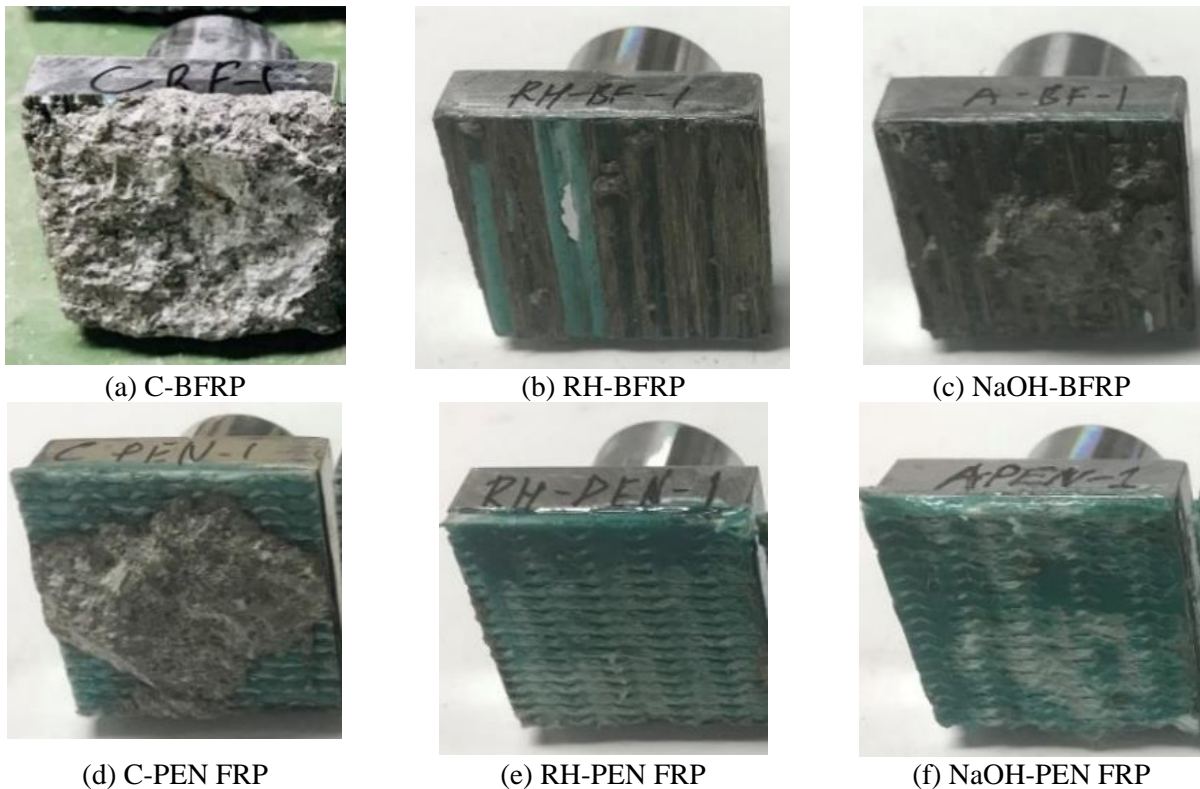

Fig. 13 Pull-off test results

(a) C-BFRP   (b) RH-BFRP   (c) NaOH-BFRP

(d) C-PEN FRP   (e) RH-PEN FRP   (f) NaOH-PEN FRP

Fig. 14 Failure mode of pull-off test specimens

Table 5 Summary of weight measured before/after exposure to wet, 3% NaCl and 1N NaOH conditions

Fiber type	Environment	Temp. (℃)	Weight before (g)	Weight after 180d (g)	Weight loss after (%)		
					30d	90d	180d
PEN fiber sheet	Wet	40	7.7040	7.6784	0.37	0.22	0.33
	NaCl	20	7.6722	7.6583	0.02	0.02	0.18
	NaOH	20	7.6815	6.8789	1.64	5.51	10.5
PEN FRP	Wet	40	11.177	11.088	0.44	--	0.80
	NaCl	20	11.007	10.924	0.16	0.05	0.76
	NaOH	20	11.083	10.602	0.73	1.70	4.34

NOTE: PEN uniaxial fiber sheet consists of 6 PEN fiber rovings; 2. Specimen length is 400 mm for PEN fiber roving, and PEN fiber sheet and 300 mm for PEN FRP; 3. Adhesive amount is 150% of fiber by vol. for PEN FRP; 4. Average of twelve measurements

Table 6 Summary of tensile test results before/after exposure to wet, 3% NaCl and 1N NaOH conditions

Fiber type	Environment	Temp. (°C)	Tensile strength before/after (MPa)				Elastic modulus before/after (GPa)			
			before	30d	90d	180d	before	30d	90d	180d
PEN fiber sheet	Wet	40		786	932	961		15.9	17.3	18.0
	NaCl	20	842	923	935	966	17.5	17.2	16.9	17.9
	NaOH	20		861	851	816		17.0	17.7	17.2
PEN FRP	Wet	40		893	902	897		20.7	19.7	21.3
	NaCl	20	912	952	935	880	21.4	20.3	20.0	21.4
	NaOH	20		857	900	844		21.9	20.3	22.2

NOTE: Average of twelve tests

(a) Control

(b) Wet

(c) 3% NaCl

(d) 1N NaOH
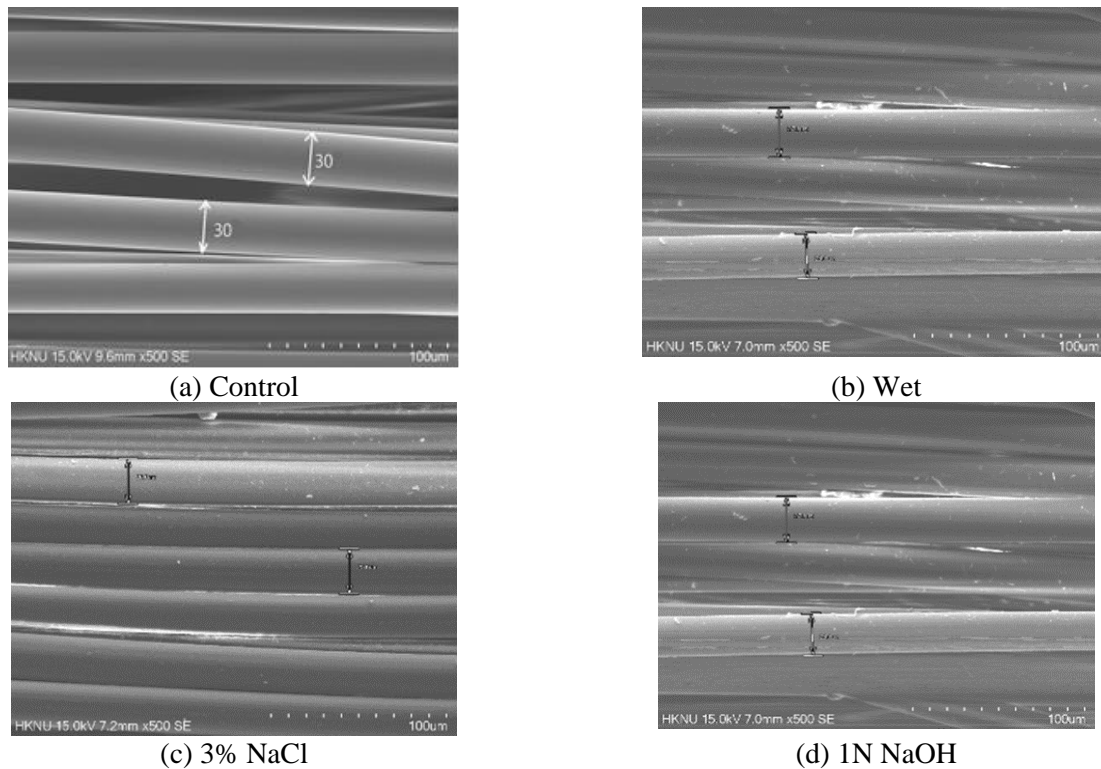
Fig. 15 SEM photos of PEN after exposure for180 days to different environmental conditions
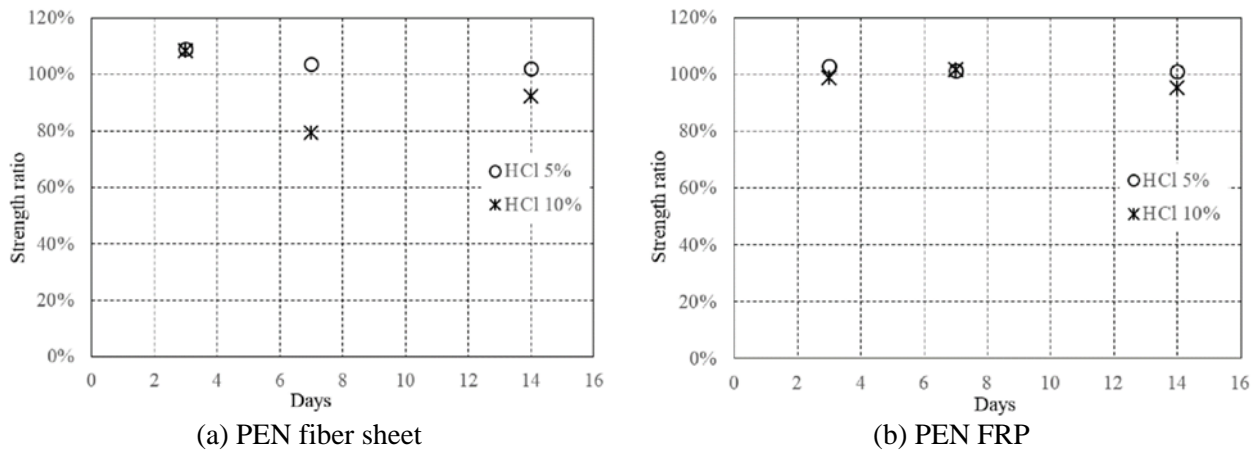
(a) PEN fiber sheet

(b) PEN FRP

Fig. 16 Results of tensile test of PEN fiber/FRP after immersion in acidic solutions

Table 7 Summary of tensile strengths for PEN FRP after exposure in natural conditions for up to 6 months

Fiber type	Before (MPa)	After 6 months (MPa)	After/Before (%)
PEN fiber sheet	842	594	70.5
PEN FRP	912	814	89.3

NOTE: Average of 10 tests

4. Conclusions

Bond between BFRP-to-concrete and PEN FRP-to-concrete interface was studied in terms of distribution and magnitude of bond stress by double lap shear test. In addition, durability characteristics of BFRP and PEN fiber/FRP have been studied by (1) beam bond test following accelerated conditioning protocols for durability assessment by ACI 440.9R, (2) fiber tensile test before/after immersion in 1N NaOH and 3% NaCl solutions, and water, (3) fiber tensile test before/after immersion in diluted acidic solutions, and (4) exposure to natural outdoor environment. The durability investigation by beam bond test included both BFRP and PEN FRP. Other durability investigations concentrated on PEN fiber/FRP. The following conclusions can be drawn from the current experimental study.

(1) Double lap shear test results show that the bond stress that develops at the interface between BFRP and concrete is relatively high and narrowly distributed: Maximum bond stress was 8.4 MPa and distance the bond stress distributed was 63-84 mm for BFRP. On the other hand, the bond stress was relatively low and distributed over a larger distance for PEN FRP: Maximum bond stress was 4.3 MPa while the distance the bond stress distributed was 105 mm for PEN FRP. Test results show that the effective bond length L_e is 84 mm for BFRP and 105 mm for PEN FRP.

(2) Beam bond test results show that the behavior of PEN FRP under wet and alkaline conditions is relatively good with beam bond retention of 88% after immersion in water and alkaline solutions for 4 months. Behavior of BFRP was not as good under alkaline environment with the beam bond retention of 51.5% after immersion for 4 months.

(3) Results of weight measurement and tensile test of PEN fiber/FRP before and after wet, alkaline, and saline conditions indicated possible degrading of PEN fiber under alkaline condition. For the PEN FRP, however, the weight reduction (about 4%) and reduction of the tensile strength was small (7.5%) and there was no change of the elastic modulus before/after immersion for 6 months.

(4) Tensile strength of PEN FRP immersed in 5% and 10% diluted acidic solutions of HCl was very good after 14 days: no reduction in 5% solution and less than 3% reduction in 10% solution. Tensile strength of PEN FRP after exposure for 6 months in natural environment showed about 10% reduction.

(5) In overall, the performance of PEN fiber/FRP was satisfactory in all durability tests conducted in this study.

Acknowledgements

Reference

1. Singha K. (2012) "A Short Review on Basalt Fiber", International Journal of Textile Science, 1(4), pp. 19-28.

2. Prasad V.V.; Talupula S. (2018) "A Review on Reinforcement of Basalt and Aramid (Kevlar 129)", Materials Today, proceedings, pp. 5993-5998, available online at www.aciencedirect.com.

3. Chen W.; Pham T.M.; Sichembe H.; Chen L.; and Hao H. (2018) "Experimental study of flexural behaviour of RC beams strengthened by longitudinal and U-shaped basalt FRP sheet", Composites Part B, 134, pp. 114-126.

4. Choobbor S.S.; Hawileh R.A.; Abu-Obeidah A.; and Abdalla J.A. (2019) "Performance of hybrid carbon and basalt FRP sheets in strengthening concrete beams in flexure", Composite Structures, 227, 111337.

5. Jiang S.-F.; Zeng X.; Shen S.; and Xu X. (2016) "Experimental studies on the seismic behavior of earthquake-damaged circular bridge columns repaired by using combination of near-surface-mounted BFRP bars with external BFRP sheets jacketing", Engineering Structures, 106, pp. 317-331.

6. Ouyang L.-J.; Gao W.-Y.; Zhen B.; and Lu Z.-D. (2017) "Seismic retrofit of square reinforced concrete columns using basalt and carbon fiber-reinforced polymer sheets: A comparative study", Composite Structures, 162, pp. 294-307.

7. Rousakis T.C.; Panagiotakis G.D.; Achiontaki E.E.; and Kostopoulos A.K. (2019) "Prismatic RC columns externally confined with FRP sheets and pretensioned basalt fiber ropes under cyclic load", Composites Part B, 163, pp. 96-106.

8. Shen D.; Shi H.; Ji Y.; and Yin F. (2015) "Strain rate effect on effective bond length of basalt FRP sheet bonded to concrete", Construction and Building Materials, 82, pp. 206-218.

9. Nerilli F.; and Vairo G. (2018) "Experimental investigation on the debonding failure mode of basalt-based FRP sheets from concrete", Composites Part B, 153, pp. 205-216.

10. Xie J.-H.; Wei M.-W.; Huang P.-Y.; Zhang H.; and Chen P.-S. (2019) "Fatigue behaviour of the basalt fiber-reinforced polymer/concrete interface under wet-dry cycling in a marine environment", Construction and Building Materials, 228, 117065.

11. Baasankhuu B. (2019) "Basic Study for Seismic Strengthening of Reinforced Concrete (RC) Structural Members Using Basalt Fiber (BF) and Ductile Polyethylene Naphthalate (PEN) ", M.S. Thesis, Hankyong National University, Anseong, South Korea.

12. Fiore V.; Bella G.D.; Valenza A. (2011) "Glass-basalt/epoxy hybrid composites for marine applications", Materials and Design, 32, pp. 2091-2099.

13. Rybin V.A.; Utkin A.V.; and Baklanova N.I. (2013) "Alkali resistance, microstructural and mechanical performance of zirconia-coated basalt fibers", Cement and Concrete Research, 53, pp. 1-8.

14. Rybin V.A.; Utkin A.V.; and Baklanova N.I. (2016) "Corrosion of uncoated and oxide-coated basalt fibre in different alkaline media", Corrosion Science, 102, pp. 503-509.

15. Anggawidjaja D.; Ueda T.; Dai J.; and Nakai H. (2006) "Deformation capacity of RC piers wrapped by new fiber-reinforced polymer with large fracture strain", Cement & Concrete Composites, 28, pp. 914-927.

16. Choi D.; Vachirapanyakun S.; Kim S.-Y.; and Ha. S.-S. (2015) "Ductile fiber wrapping for seismic retrofit of reinforced concrete columns", Journal of Asian Concrete Federation, 1(1), pp. 37-46.

17. Dai, J.-G.; Bai, Y.-L.; and Teng, J. G. (2011) "Behavior and modelling of concrete confined with FRP composites of large deformability", ASCE Journal of Composites for Construction, 15(6), pp. 963–973.

18. Baasankhuu B.; Choi D.; and Ha S.S. (2020) "Behavior of Small-Scale Concrete Cylinders in Compression Laterally Confined by Basalt Fiber and PEN Fiber Reinforced Polymer Composites", IJCSM, 14(8), pp. 1-19.

19. Saleem S.; Pamanmas A.; and Rattanapitikon W. (2018) "Lateral response of PET FRP-confined concrete", Construction and Building Materials, 159, pp. 390-407.

20. Suon S.; Saleem S.; and Pimanmas A. (2019) "Compressive behavior of basalt FRP-confined circular and non-circular concrete specimens", Construction and Building Materials, 195, pp. 85-103.

21. Park H.S.; Kim S.Y.; Lim M.K.; and Choi D. (2016) "Bond and Flexural behaviour of RC Beams Strengthened Using Ductile PET, Journal of the Korea Institute for Structural Maintenance and Inspection", 20(6), pp. 30-39. (in Korean)

22. ISO 10406-2 (2015) "Fiber reinforced polymer (FRP) reinforcement of concrete – Test methods - Part 2: FRP sheets", International Organization for Standardization, Geneva, Switzerland.

23. ASTM D 638-08 (2008) "Standard Test Method for Tensile Properties of Plastics", American Society of Testing and Materials, West Conshohocken, PA.

24. Teng J.G.; Chen J.F.; Smith S.T.; and Lam L. "FRP Strengthened RC Structures", Wiley, 2002.

25. Choi, D.-U.; Fowler, D.W.; and Wheat, D.L. (1996) "Thermal Stresses in Polymer Concrete Overlays", American Concrete Institute, Special Publication SP-166, Properties and Uses of Polymers in Concrete, pp. 93-122.

26. CSA S806-02 (2002) "Design and Construction of Building Components with Fibre-Reinforced Polymers", Canadian Standards Association, Toronto, Ontario.

27. ACI 440.9R-15 (2015) "Guide to Accelerated Conditioning Protocols for Durability Assessment of Internal and External Fiber Reinforced Polymer (FRP) Reinforcement", ACI Committee 440, American Concrete Institute, Detroit, Michigan.